

Effects of partial cross sections on the energy distribution of slow secondary electrons*

Henry C. Tuckwell† and Yong-Ki Kim

Argonne National Laboratory, Argonne, Illinois 60439
(Received 8 September 1975)

The shapes of the energy distribution of secondary electrons can be predicted for fast incident charged particles by using dipole oscillator strengths in conjunction with the Born formula. Target atoms or molecules may have one or more ionization potentials close to the first one and the corresponding partial photoionization cross sections are sometimes large. Allowance must then be made for the differences in kinetic energies of photoelectrons which leave alternative ionic states. This produces a significant change in the expected secondary electron spectrum at low energies. The photoionization data for NO are analyzed and the predicted shape of the secondary electron energy distribution agrees well with that of the experimental distribution at those secondary electron energies where a comparison is possible. Predicted low energy results from a preliminary analysis for N₂ are also reported.

I. INTRODUCTION AND THEORY

In previous papers¹⁻³ a method was given for testing the consistency of experimentally determined energy distributions of secondary electrons produced by the impact of fast charged particles on atoms or molecules. The method is based on the formula for the differential cross section in the first Born approximation which for incident particles of charges ze and velocity v is given by¹

$$\left. \frac{d\sigma(E, T)}{dE} \right|_{\text{Born}} = \frac{4\pi a_0^2 z^2}{T} \left\{ A(E) \ln \left[\frac{4TRC(E)}{E^2} \right] + B(E, T) \right\}, \quad (1)$$

where $T = \frac{1}{2}mv^2$, m being the electronic mass, a_0 is the Bohr radius, R is the Rydberg unit, and E is the energy transfer. The function $C(E)$ is the square of the maximum momentum transfer at which the dipole interaction dominates, $A(E)$ is related to the dipole oscillator strength df/dE through the relation

$$A(E) = \frac{R^2}{E} \frac{df(E)}{dE}, \quad (2)$$

and $B(E, T)$ contains the contributions to $d\sigma/dE$ from "hard" collisions, i. e., those with large momentum transfers. If the target electrons have binding energy B , then the secondary electron energy is $W = E - B$. If there are several binding energies, then there will be summations over the contributions from different orbitals in Eq. (1).

For the production of fast secondary electrons, hard collisions dominate, and the main features of the differential cross section can be obtained from the Mott formula for incident electrons or the Rutherford formula for other particles.⁴ At low and intermediate secondary energies where "soft" collisions (i. e., those with small momentum transfers) are more prevalent, the characteristics of $d\sigma/dE$ as a function of E are mainly determined by those of df/dE . The above approach has been verified for many collision systems, e. g., for proton and electron impact data for He,⁵ and electron impact data for Ar,^{1,6} H₂,⁷ and Ne.⁸ Some workers have, in fact, introduced "empirical" scaling functions to weight the hard and soft collision contributions in the Born formula.^{6,7,9}

It has proved valuable to present secondary electron data by means of a Platzman plot in which the quantity

$$Y(E, T) = \frac{d\sigma(E, T)}{dE} \frac{TE^2}{4\pi a_0^2 R^2} \quad (3)$$

is plotted against the inverse of the energy transfer in Rydbergs. The quantity $Y(E, T)$ is, in fact, the ratio of the differential cross section to that given by the Rutherford formula. The advantages of presenting the data in such a fashion are (1) the range of the independent variable (R/E) is finite, (2) the low and intermediate energy parts of the spectrum are emphasized, and (3) the area under the curve is proportional to the total ionization cross section. In particular, (2) and (3) enable one to test the consistency of the data in the way described in previous articles.¹⁻³

Thus, if one inserts the Born formula¹ in Eq. (3), the dipole contribution appears as $E df/dE$. Since low and intermediate energy secondaries are produced (for high incident energy T) mainly by the dipole interaction, part (2) of the consistency test can be performed by comparing the shape of $Y(E, T)$ with that of $E df/dE$ in the Platzman plot. Values of the latter can be obtained from measured total photoionization cross sections $\sigma_{\text{ph}}(E)$ through the relation

$$\sigma_{\text{ph}}(E) = 4\pi^2 \alpha a_0^2 R [df(E)/dE], \quad (4)$$

where α is the fine structure constant.

In all the previous applications of the above approach, the formulas (2) through (4) have been used without taking into account the various ionization potentials of the target atom or molecule. In secondary electron spectra only the kinetic energy of the electrons is taken into account, not the energy transfer. That is, electrons with a given kinetic energy could have come from various orbitals with different binding energies. Photoionization cross sections, on the other hand, are usually reported as functions of the photon energy E (or wavelength) which is the actual energy transferred in the ionization process. Since we are interested in comparing the continuum oscillator strength with the secondary electron energy distribution, we have to recast the former as a function of the kinetic energy of the ejected electrons.

Suppose an atom or molecule has a sequence of ionization potentials B_j , for $j=1, 2, \dots, n$. We distinguish the corresponding partial oscillator strengths for ionization, df_j/dE_j , where $E_j = W + B_j$, from the total oscillator strength for ionization, df/dE . When summation over different orbitals is taken into account in the Born formula (1), it is apparent that the dipole contribution to $Y(E, T)$ comes from

$$F(W) = \frac{E df_1}{dE} + \sum_{j=2}^n \frac{E^2}{E_j} \frac{df_j(E_j)}{dE_j}, \quad (5)$$

where $E = W + B_1$. It is the shape of $F(W)$ in the Platzman plot which should indicate the shape of $Y(E, T)$ for low and intermediate values of E . [Note that the total areas under the curves $F(W)$ and $E df/dE$ are identical in the Platzman plot providing one neglects multiple ionization.]

Let $\Delta_j = B_j - B_1$ for $j=2, \dots, n$. When the Δ_j are large and the corresponding partial photoionization cross sections are small in comparison with the total cross section, the partitioning of df/dE is not important, as illustrated by the previous analyses⁸ for Ne, etc. For atoms of large atomic number and for most diatomic molecules other than H_2 , the first few Δ_j may be quite small, and the partial cross sections for transitions leading to the first few excited ionic states are often quite large, in which case the quantity $F(W)$ departs significantly from $E df/dE$. This will be illustrated for the molecule NO for which a substantial amount of data are available concerning ionization potentials and partial cross sections. A brief qualitative report of our analysis for N_2 will also be given.

TABLE I. Ionization potentials of NO.

M.O. of NO vacated	State of NO*	Ionization potential (eV)	Group
$\pi_g 2p$	$X' \Sigma^+$	9.26 ^a	X
$\pi_g 2p$	$a^3 \Sigma^+$	15.65 ^a	A
	$w^3 \Delta$	16.84 ^a	B
	$b^3 \Sigma^-$	17.55 ^a	B
	$A' ^1 \Sigma^-$	18.39 ^a (17.8) ^b	B
	$W^1 \Delta$	19.28 ^a (18.1) ^b	B
	$B' ^1 \Sigma^+$	23.3 ^c	D
$\sigma_g 2p$	$b^3 \Pi$	16.54 ^a	A
	$A^1 \Pi$	18.30 ^a	B
$\sigma_u 2s$	$c^3 \Pi$	20.4 ^b	C
	$B^1 \Pi$	21.72 ^b	C
$\sigma_g 2s$	$^3 \Pi$	23.1 ^d	D
	$^1 \Pi$	23.3 ^e	D

^aReference 10.

^bReference 11.

^cVertical I. P. (Ref. 11).

^dReference 12.

^eReference 13.

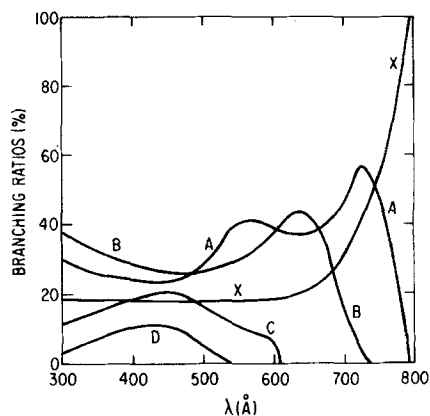


FIG. 1. Branching ratios versus photon wavelength for production of states of groups of states of NO^+ by photoionization of NO. For details of the groups of states, see Table I.

II. APPLICATION TO NO

The diatomic molecule NO has several ionization potentials within 10 eV of the first ionization potential (9.26 eV) and the partial cross sections for photoionization leading to excited states of NO^+ have high branching ratios. Hence, this molecule is one for which recasting the $E df/dE$ curve according to Eq. (5) should be important. This is also expected to be the case for large atoms such as Xe, the diatomic molecules N_2 , O_2 , and CO, as well as polyatomic molecules such as H_2O , CH_4 , and NH_3 . For many of these, however, there are insufficient data on partial cross sections to carry out the necessary computations. For NO, the reconstitution of $E df/dE$ produces significant changes well into the energy region of the measured secondary electron spectrum and a direct test of the importance of the use of Formula (5) is possible.

The ground state of NO has the electronic structure which can be written¹⁰ (though the g and u symmetries are not strict)

$$X^2 \Pi: KK(\sigma_g 2s)^2 (\sigma_u 2s)^2 (\sigma_g 2p)^2 (\pi_u 2p)^4 (\pi_g 2p)^1.$$

Table I shows the 13 states of NO^+ which result when various orbitals higher than the K shells (denoted by KK) are vacated, together with the corresponding ionization potentials. The values are taken from Turner *et al.*,¹⁰ Edqvist *et al.*,¹¹ Samson,¹² and Siegbahn *et al.*¹³ The Turner *et al.* values are given when they are close to the values given by Edqvist *et al.* If there is a large discrepancy, then the Edqvist *et al.* value is given in parentheses. The next ionization potential below those given in Table I is 40.6 eV¹³ corresponding to a wavelength of 305 Å.

Partial photoionization cross sections for NO have been measured from 584 to 792 Å by Bahr *et al.*,¹⁴ but some ionic states are not resolved when their ionization potentials are close. Groups of such close-lying final states for which partial cross sections are not resolved are classified as A, B, C, and D in Table I. The only other available partial cross section data are at 462 Å¹² and at 304 Å.¹¹ These three sets of data were used to construct the branching ratio curves for production of states or groups of states of NO^+ shown in Fig. 1. It

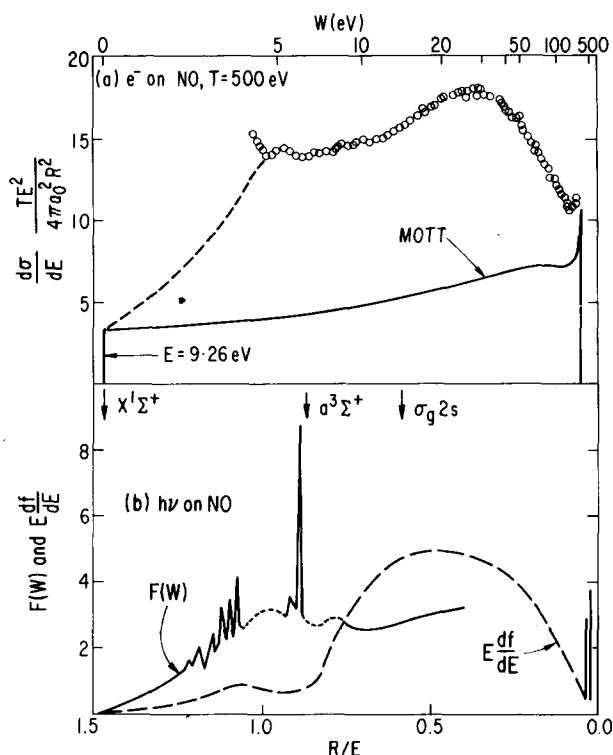


FIG. 2. (a) The Platzman plot for 500 eV electron impact on NO. The circles represent the electron-impact data by Opal *et al.*¹⁶. The solid curve is the result from the version of the Mott formula employed previously.¹⁻³ The dashed curve is the extrapolation of the Opal *et al.* data based on the shape of the quantity $F(W)$ shown in Fig. 2(b). (b) The long dashed curve is a plot of $E df/dE$ versus inverse energy transfer from photoionization data (see text). The vertical lines near $R/E=0$ correspond to K -shell absorption. The (mainly) solid curve is a plot of the quantity $F(W)$ [Eq. (5)]. In the (short) dashed portions of this curve are many closely spaced autoionization peaks.

can be seen that contributions to the total cross section from groups A and B become larger within a few eV of their appearance thresholds. Though there are uncertainties in the details of these curves below 584 Å, the most important effects in the reconstituted oscillator strength density come from energies where the branching ratios are known.

The partial cross sections (df_j/dE_j) to be used in Eq. (5) should be independent of the angular distribution of photoelectrons since we are interested only in the energy distribution of secondary electrons. Unfortunately, most data on partial cross sections determined from photoelectron analysis, including those in Refs. 11 and 14, are deduced from photoelectrons ejected at 90° to the incident light beam direction. Partial cross sections obtained by integration over the photoelectron angles may be somewhat different from those at 90°. Hence, our results on $F(W)$ presented below may require slight modification if data on partial cross sections that are angle-independent become available (e.g., by measurements at the "magic angle").

In Fig. 2(b) is shown the $E df/dE$ curve obtained from the photoionization data compiled by Berkowitz.¹⁵ In the wavelength range from first threshold to about 680 Å the

photoionization cross section is characterized by a large number of autoionization peaks corresponding to Rydberg series converging to excited states of NO^+ . An estimate of the direct photoionization contribution was made by drawing a smooth curve through the lowest points (long dashed curve).

The branching ratios of Fig. 1 were applied to values of the total df/dE , and $F(W)$ [Eq. (5)] was computed at various values of the energy transfer up to $E = 2.5 R$. The results are indicated by the (mainly) solid curve in Fig. 2(b). Extrapolation of known branching ratios was necessary for a few high E values when calculating the contributions from transitions which lead to highly excited states of NO^+ , but the uncertainties in the final results should not be more than 10%. Some of the pronounced autoionization peaks have been included in the term $E df/dE$, but there are so many in the region from $E = 0.95$ to $1.35 R$ that a dashed curve has been used in Fig. 2(b) for most of that energy region. Furthermore, when autoionization could leave the ion in either the ground or excited states [i.e., when E is greater than the appearance potential of NO^+ ($a^3\Sigma^+$)], the kinetic energies of the ejected electron can be determined only when branching ratios are known. The correct magnitudes and energies of the autoionization peaks for $E > 1.15 R$ are thus uncertain, but the details of those peaks which have been included are accurate.

The outline of the theory in Sec. I indicated that the differential cross section for production of secondary electrons should consist of soft and hard collision components. The version of the Mott formula previously employed¹⁻³ was used to compute the curve marked "MOTT" in Fig. 2(a). For NO one must take into account the degeneracy in the final states which result when an electron is removed from $\pi_u 2p$ orbitals. Also shown in Fig. 2(a) is the Platzman plot of the secondary electron data of Opal *et al.*¹⁶ for impact of 500 eV electrons on NO.

It can be seen that "adding" the original $E df/dE$ value in Fig. 2(b) to the Mott curve of Fig. 2(a) would lead to a sharper rise of $Y(E, T)$ at $R/E = 0.85 R$ than that of the Opal *et al.* data.¹⁶ Furthermore, the peak would be at the wrong secondary electron energies. The result of adding the calculated $F(W)$ to the Mott cross section, on the other hand, leads to a shape which is in agreement with the secondary electron data where this is known. Also, $Y(E, T)$ for the experimental data begins to turn upward at the lowest secondary energies for which the cross section was measured. One can see that this is not the beginning of an overall trend, but probably a superposition of autoionization peaks. Further confirmation of this is obtained by extrapolating $Y(E, T)$ from the Opal *et al.* data to zero secondary kinetic energy according to the shape of $F(W)$. This is indicated by the dashed curve in Fig. 2(a). That this extrapolated $Y(E, T)$ is basically correct is obtained by determining the value of the total ionization cross section σ_i from the relation

$$\frac{\sigma_i(T)}{4\pi a_0^2} = \frac{z^2 R}{T} \int_{R/E_{\text{max}}}^{R/B_1} Y(E, T) d(R/E), \quad (6)$$

where $E_{\max} = (T - B_1)/2$. From the Opal *et al.* data¹⁶ and the extrapolated $Y(E, T)$ in Fig. 2(a), one obtains $\sigma_i = 1.95 \pi a_0^2$ (without autoionization peaks) which agrees well with the experimental value of $\sigma_i = 2.10 \pi a_0^2$ obtained by Rapp and Englander-Golden.¹⁷

The results we have given for NO show that when there are ionization potentials close to the first and the partial photoionization cross sections for production of the corresponding excited ionic states are large, then it is important to recast the $E df/dE$ curve to allow for the different kinetic energies of the ejected electrons. The method employed previously for light rare gas atoms and H_2 , using the Born formula (1) in conjunction with oscillator strength data and a hard collision cross section (Mott or Rutherford), can then be applied to more complex atomic or molecular systems, providing partial cross sections are known over a sufficient range of energies. More experiments on partial cross sections, for E up to 100 eV, are clearly desirable. Although the branching ratios for NO below 584 Å in Fig. 1 have been interpolated using the few known data points, the gross features of $F(W)$ are expected to be basically correct. The use of correct partial cross sections in the calculation of average energy spent per ion pair, for example, would lead to a higher value than that obtained from the total $E df/dE$.

Finally, we make some remarks about our investigation for N_2 . Though the partial cross section data are not as well known for this molecule as NO, we used the available data to calculate the quantity $F(W)$ from the measured total photoionization cross sections of Cook and Metzger¹⁸ and the values given by Berkowitz¹⁵ in conjunction with the partial cross sections obtained by Blake and Carver¹⁹ and by Gardner and Samson.²⁰ The most significant differences between $E df/dE$ and $F(W)$ occurred between first threshold ($E = 1.15$ R) and $E = 1.55$ R, where a comparison with the value $Y(E, T)$ of the Opal *et al.* data¹⁶ is not possible. Our computed $F(W)$ values indicate that $d\sigma/dE$ should have a peak for secondary electron energies of about 1.1 eV and a minimum at about 2.9 eV. The data of Stolterfoht²¹ for proton impact on N_2 show the predicted peak at the correct secondary energy. The minimum, however, is not discernible in the experimental results, which could be due to its being filled in by closely spaced autoionization peaks. Additional data are needed to completely resolve the discrepancy.

ACKNOWLEDGMENTS

The authors wish to thank Dr. J. Berkowitz for providing photoionization and photoabsorption cross sections. One of the authors (HCT) is grateful to Dr. M. Inokuti for his hospitality and many interesting discussions.

*Work performed under the auspices of the U. S. ERDA.

†Present address: Dept. of Mathematics, University of British Columbia, Vancouver, B. C., Canada.

¹Y.-K. Kim, *Radiat. Res.* **61**, 21 (1975).

²Y.-K. Kim, *Radiat. Res.* **64**, 96 (1975).

³Y.-K. Kim, *Radiat. Res.* **64**, 205 (1975).

⁴L. Landau and E. M. Lifshitz, *Quantum Mechanics. Non-relativistic Theory* (Pergamon, London, 1965), 2nd ed., p. 575.

⁵Y.-K. Kim and T. Noguchi, *Int. J. Radiat. Phys. Chem.* **7**, 77 (1975).

⁶E. Eggarter, *J. Chem. Phys.* **62**, 833 (1975).

⁷D. E. Gerhart, *J. Chem. Phys.* **62**, 821 (1975).

⁸Y.-K. Kim, in *Invited Lectures and Progress Reports, IXth International Conference on Electronic and Atomic Collisions, Seattle*, edited by J. S. Risley, and R. Geballe (University of Washington, Seattle, 1976).

⁹R. Shingal, B. B. Srivastava, and S. P. Khare, *J. Chem. Phys.* **61**, 4656 (1974).

¹⁰D. W. Turner, C. Baker, A. D. Baker, and C. R. Brundle, *Molecular Photoelectron Spectroscopy* (Wiley-Interscience, New York, 1970).

¹¹O. Edqvist, E. Lindhold, L. E. Selin, H. Sjögren, and L. Asbrink, *Ark. Fys.* **40**, 433 (1970).

¹²J. A. R. Samson, *Phys. Lett. A* **28**, 391 (1968).

¹³K. Siegbahn *et al.*, *ESCA Applied to Free Molecules* (North Holland, Amsterdam, 1969).

¹⁴J. L. Bahr, A. J. Blake, J. H. Carver, J. L. Gardner, and V. Kumar, *J. Quant. Spectrosc. Radiat. Transfer* **12**, 59 (1972).

¹⁵J. Berkowitz (private communication).

¹⁶C. B. Opal, E. C. Beaty, and W. K. Peterson, *At. Data* **4**, 209 (1972).

¹⁷D. Rapp and P. Englander-Golden, *J. Chem. Phys.* **43**, 1464 (1965).

¹⁸G. R. Cook and P. H. Metzger, *J. Chem. Phys.* **41**, 321 (1964).

¹⁹A. J. Blake and J. H. Carver, *J. Chem. Phys.* **47**, 1038 (1967).

²⁰J. L. Gardner and J. A. R. Samson, *J. Electron. Spectros. Rel. Phenom.* **2**, 253 (1973). The corrected values of the branching ratios at 304 Å provided by the authors were used in estimating $F(W)$.

²¹N. Stolterfoht, *Z. Phys. (Leipzig)* **248**, 92 (1971).